Genesis of the IIICD iron meteorites: Evidence from silicate-bearing inclusions

TIMOTHY J. MCCOY, KLAUS KEIL[1], EDWARD R. D. SCOTT[1] AND HENNING HAACK

Planetary Geosciences, Department of Geology and Geophysics, School of Ocean and Earth Science and Technology
University of Hawaii at Manoa, Honolulu, Hawaii 96822, USA
[1]Also associated with the Hawaii Center for Volcanology

Abstract—Our studies of the silicate-bearing inclusions in the IIICD iron meteorites Maltahöhe, Carlton and Dayton suggest that their mineralogy and mineral compositions are related to the composition of the metal in the host meteorites. An inclusion in the low-Ni Maltahöhe is similar in mineralogy to those in IAB irons, which contain olivine, pyroxene, plagioclase, graphite and troilite. With increasing Ni concentration of the metal, silicate inclusions become poorer in graphite, richer in phosphates, and the phosphate and silicate assemblages become more complex. Dayton contains pyroxene, plagioclase, SiO_2, brianite, panethite and whitlockite, without graphite. In addition, mafic silicates become more FeO-rich with increasing Ni concentration of the hosts. In contrast, silicates in IAB irons show no such correlation with host Ni concentration, nor do they have the complex mineral assemblages of Dayton. These trends in inclusion composition and mineralogy in IIICD iron meteorites have been established by reactions between the S-rich metallic magma and the silicates, but the physical setting is uncertain. Of the two processes invoked by other authors to account for groups IAB and IIICD, fractional crystallization of S-rich cores and impact generation of melt pools, we prefer core crystallization. However, the absence of relationships between silicate inclusion mineralogy and metal compositions among IAB irons analogous to those that we have discovered in IIICD irons suggests that the IAB and IIICD cores/metallic magmas evolved in rather different ways. We suggest that the solidification of the IIICD core may have been very complex, involving fractional crystallization, nucleation effects and, possibly, liquid immiscibility.

INTRODUCTION

Analyses of Ni and siderophile trace element concentrations among iron meteorites have led to the recognition of 13 iron meteorite groups (*e.g.*, Malvin *et al.*, 1984). Eleven of these groups exhibit small ranges in Ga and Ge concentrations (Fig. 1) and are thought to have formed by fractional crystallization of 11 individual asteroidal cores; they have been referred to as the magmatic iron meteorite groups (*e.g.*, Wasson *et al.*, 1980). In contrast, group IIICD and IAB irons exhibit large, correlated variations of Ga, Ge and Ni concentrations (Fig. 1) and smaller ranges for Au and As and some authors argue they formed by a different process (Wasson, 1985). Many IABs and a few IIICDs contain silicate-bearing inclusions. Although most of these inclusions are largely dominated by troilite, graphite, phosphates or schreibersite, as a matter of convenience, we refer to them as silicate inclusions. It is difficult to ascertain why low-density silicate inclusions did not separate from high-density metal while the latter was molten, and how highly fractionated material such as the metallic Fe,Ni of iron meteorites could be mixed with silicates of essentially undifferentiated, chondritic parentage.

We report here the results of our studies of the three known silicate-bearing IIICDs, Maltahöhe (11.4 ± 1 wt% Ni; J. T. Wasson, pers. comm., 1993), Carlton (13.0% Ni; Wasson and Schaudy, 1971) and Dayton (17.0% Ni; Wasson and Schaudy, 1971). These have been plotted in Fig. 1 within the field of IIICDs. We also compare IIICD to IAB irons, in the hope that we can shed some light on their origin and evolution.

PREVIOUS WORK ON IIICD IRONS

Wasson and Schaudy (1971) were the first to classify iron meteorites into groups IIIC (11–13% Ni) and IIID (16–23% Ni) and suggested that they may be related. Scott and Bild (1974) plotted the IIICDs as a single group in diagrams of Ni *vs.* Ga and Ge. Wasson *et al.* (1980) raised the membership to 18 by including six low-Ni meteorites that had previously been classified as IABs; Hoashi *et al.* (1992) dispute these changes. None of these low-Ni members contain silicate inclusions, and they shall not be considered further in this work. Recent recoveries (Graham, 1988; Wlotzka, 1991), including that of the silicate-bearing

meteorite Maltahöhe, raise the total number of IIICDs to 20. Metallographic descriptions of most of these meteorites are given by Buchwald (1975).

There are few published studies of silicate inclusions in IIICDs. Descriptions of those in Carlton and Dayton (Fuchs *et al.*, 1967; Scott and Bild, 1974; Kracher and Kurat, 1977; Prinz *et al.*, 1982) are quite
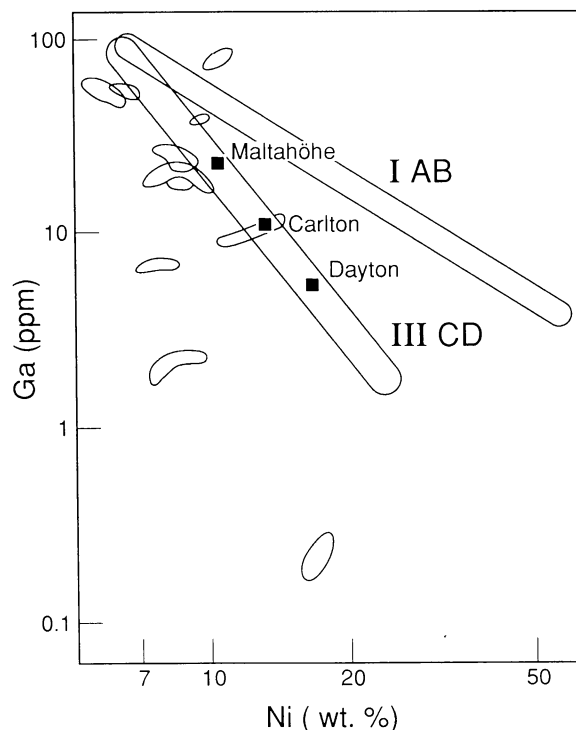

FIG. 1. The 13 iron meteorite groups depicted in a log-log plot of Ga (ppm) *vs.* Ni (wt%) (modified from Fig. II-10 in Wasson, 1985). The 11 magmatic iron meteorite groups (unlabelled outlines) have small ranges for both elements, reconcilable with fractional crystallization of the metal cores of 11 asteroidal parent bodies. In contrast, IAB and IIICD irons show enormous trace element and large Ni ranges, suggesting that they did not form by simple fractional crystallization of metal cores. The silicate-bearing IIICDs Maltahöhe, Carlton and Dayton are also plotted (see text for sources of data).

brief, and inclusions in Maltahöhe are undescribed. The only published picture of IIICD silicates is that of a hand sample of Maltahöhe (Spratt and Stephens, 1992), and the only oxygen isotopic measurements of IIICDs are those of phosphates in Dayton (Clayton *et al.*, 1983), which suggest a close relationship between IIICDs and IABs. Data which have played key roles in models on the genesis of IABs, such as ages (*e.g.*, Niemeyer, 1979a,b) and REE (*e.g.*, Bild, 1977) and noble gas abundances (*e.g.*, Hintenberger *et al.*, 1969), are unavailable for inclusions in IIICDs. Presumably, this is because such inclusions are very small and rare.

ANALYTICAL TECHNIQUES

A single, large inclusion from Maltahöhe (PTS UH 185) was examined, and polished thick sections of Carlton (USNM 2707) and Dayton (USNM 1592) were studied. We have defined the boundary of these inclusions to extend to all phases associated with the silicates and contained within Fe,Ni metal. We recognize that this definition is somewhat arbitrary and includes phases which exsolved from the solid after crystallization (*e.g.*, schreibersite).

A search for silicate-bearing inclusions in the Edmonton (Kentucky) iron was unsuccessful. Ramdohr (1973) reported the existence of such an inclusion in a section from the Max-Planck-Institut in Heidelberg, but this section appears lost. The only silicate material identified (in polished section USNM 1413) is of terrestrial origin.

Optical microscopy and modal analyses were performed on a Nikon photomicroscope equipped for both transmitted and reflected light. No attempt was made to distinguish silicate phases during modal analyses. Analyses of individual phases, except phosphates, were made with a Cameca Camebax electron microprobe operated at an accelerating voltage of 15 keV and an absorbed sample current of 15 nA for most phases (10 nA for plagioclase). A 10 μm beam was used for plagioclase analyses. Natural and synthetic standards of well-known compositions were used, and data were corrected using a ZAF program. Phosphate analyses were performed on a Cameca SX-50 electron microprobe at an accelerating voltage of 15 keV, an absorbed current of 10 nA and a 10 μm beam. Natural and synthetic standards were used, and data were corrected by the PAP $\phi(\rho z)$ program.

RESULTS

Maltahöhe

The Maltahöhe iron contains 11.4 wt% Ni and was found in 1991 (Wlotzka, 1991). An etched slice shows prominent, abundant (14 vol%), irregularly-shaped graphite-troilite-silicate inclusions (Fig. 2). We have studied a single 14 by 7 mm silicate-bearing inclusion (Fig. 3), which appears similar in size, shape and mineralogy to numerous other inclusions in hand sample. This inclusion is dominated by troilite, graphite, silicates and schreibersite (Table 1). No phosphates and only rare chromite were observed. Silicates (olivine, pyroxene, plagioclase) occur as mono- or poly-mineralic clusters. The inclusion has a generally concentric structure, with graphite more abundant in the interior and troilite more abundant at the edges. Within and bordering the metallic host, the cliftonite variety of graphite is found, with its distinctive cube shape. Graphite also occurs as laths which protrude into the metal, giving the metal-graphite interface a serrated appearance. Olivine grains, up to a few millimeters in size, sometimes poikilitically enclose pyroxene. Petrographic features which are diagnostic of shock (*e.g.*, undulatory extinction, planar fractures; Stöffler *et al.*, 1991) are absent from olivine grains. Schreibersite grains are confined to the margins of the inclusion.

Olivines have an average composition of $Fa_{5.0 \pm 0.4}$ (Table 2). Reduction is indicated by slight inverse zoning of individual grains (Fig. 4) and by the pyroxene composition of $Fs_{7.8 \pm 0.2}$, which is higher than the Fa content, apparently reflecting disequilibrium between the two phases (*e.g.*, Bowen and

FIG. 2. Hand sample of the Maltahöhe iron meteorite (~15 cm long). Graphite-troilite-silicate inclusions (dark) comprise 14.4% of the surface area. The inclusions are irregularly shaped, similar to Odessa-type inclusions from IAB irons. Sample from the Robert Haag collection.

Schairer, 1935). Plagioclase grains also show a range of compositions ($An_{0.1 \pm 0.1 - 13.6}$, mean $An_{3.4 \pm 4.0}Or_{3.5 \pm 0.7}$), indicating local disequilibrium.

Carlton

The Carlton meteorite (13.0 wt% Ni) has been described by Buchwald (1975). Kracher and Kurat (1977) and Prinz *et al.* (1982) reported rare silicate inclusions rich in olivine, pyroxene and plagioclase. Kracher and Kurat (1977) noted troilite-rich areas and rims of radially crystallized graphite around isolated silicate grains; Prinz *et al.* (1982) observed minor (0.8 vol%) farringtonite. Our examination of numerous slices of Carlton and published photos suggest that silicate-bearing inclusions comprise much less than 1% of the bulk meteorite.
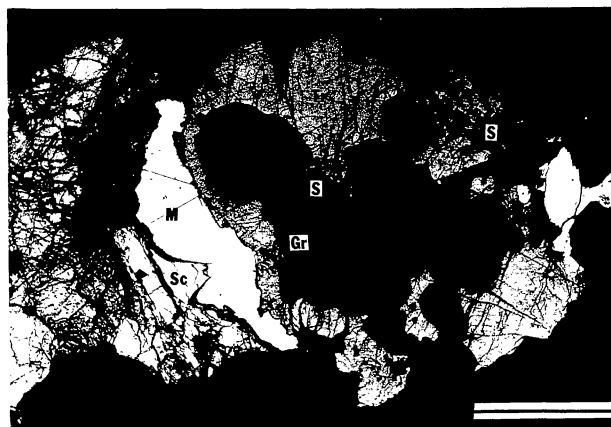

FIG. 3. Reflected light photomicrograph of an inclusion in Maltahöhe. Silicate phases (S) are olivine, pyroxene and plagioclase. The matrix is dominantly graphite (Gr) in the center and troilite (Tr) at the edge. Schreibersite (Sc) occurs bordering the Fe,Ni metal (M) host. This inclusion is very similar in mineralogy and texture to Odessa-type inclusions in IAB irons. Scale bar = 2 mm.

McCoy *et al.*

TABLE 1. Modal analyes of silicate inclusions in IIICD iron meteorites (in vol%). Fe,Ni was excluded from the analyses.

Mineral	W. S.†	Maltahöhe			Carlton			Dayton
		#1	#2	#3	#1	#2	#3	
Silicates	13.9	26.6	55.6	12.8	6.0	5.5	12.7	
Phosphates								
Whitlockite	--	--	--	--	14.6	--	--	
Chlorapatite	--	--	--	69.8	--	--	--	
Brianite	--	--	--	--	22.1	16.5	0.8	
Panethite	--	--	--	--	17.9	5.8	--	
N. P.‡	--	--	--	0.5	--	--	--	
Schreibersite	9.7	73.3	17.2	3.9	19.6	53.7	83.2	
Troilite	42.9	--	--	--	17.3	18.2	3.3	
Fe,Ni-FeS Intergrowth	--	--	6.7	12.7	--	--	--	
Graphite	25.4	--	3.7	--	--	--	--	
W. P.*	7.5	--	16.5	--	--	--	--	
Copper	--	--	--	--	0.2	--	--	
Sphalerite	--	--	--	--	2.0	--	--	
Chromite	0.2	--	--	--	--	--	--	
No. of Points	1178	30	133	918	479	1172	387	

† Whole Section
‡ New Phosphate
* Weathering Products

The sample we studied measures 2.5 x 1.6 cm and has an irregular outline. Three irregularly-shaped inclusions, the largest of which is 5 x 5 mm, comprise 17% of the surface of this piece. Olivine, pyroxene and plagioclase occur as mono- or polymineralic clusters in a matrix which differs between inclusions, and schreibersite is omnipresent. In the two largest inclusions, there are intergrowths of μm-sized Fe,Ni metal and troilite, which we believe formed by shock melting. However, R. S. Clarke, Jr. (pers. comm., 1993) suggests that the intergrowth results from ablation heating rather than shock, since it lies within the heat-affected zone. FeO contents of pyroxenes are higher than those of olivines in all three inclusions. The average olivine composition of $Fa_{6.8 \pm 0.4}$ (N = 17) is similar to that reported by Kracher and Kurat (1977) ($Fa_{6.5}$), but differs significantly from the value of Prinz *et al.* (1982) (Fa_9); we detected no olivines of Fa_9, although we have not analyzed the samples studied by Prinz *et al.* (1982).

TABLE 2. Compositions of minerals from silicate inclusions in IIICD irons.

Meteorite	IC†	Olivine		Pyroxene			Plagioclase		
		N	Fa	N	Fs	Wo	N	An	Or
BY INCLUSION									
Maltahöhe	Entire	10	5.0 ± 0.4	10	7.8 ± 0.2	1.7 ± 1.2	10	3.4 ± 4.0	3.5 ± 0.7
Carlton	#1	2	6.6 ± 0.1	2	9.7 ± 0.3	1.3 ± 0.1	1	0.8	4.1
	#2	7	6.6 ± 0.2	8	9.7 ± 0.6	1.3 ± 0.4	7	5.2 ± 1.4	3.4 ± 0.7
	#3a	5	6.7 ± 0.3	4	9.8 ± 0.1	1.7 ± 0.3	4	6.3 ± 3.3	3.3 ± 0.9
	#3b	3	7.5 ± 0.5	5	9.5 ± 0.4	1.6 ± 0.2	5	4.0 ± 2.7	4.0 ± 0.8
Dayton	#1	–	–	13	11.8 ± 1.0	0.9 ± 0.3	6	0.7 ± 0.8	1.8 ± 0.4
	#2	–	–	9	11.5 ± 0.7	0.8 ± 0.2	5	1.1 ± 1.7	1.9 ± 0.3
	#3	–	–	6	11.6 ± 0.8	1.0 ± 0.6	7	1.3 ± 1.4	2.0 ± 0.5
METEORITE AVERAGE									
Maltahöhe	Aver.	10	5.0 ± 0.4	10	7.8 ± 0.2	1.7 ± 1.2	10	3.4 ± 4.0	3.5 ± 0.7
Carlton	Aver.	17	6.8 ± 0.4	19	9.7 ± 0.5	1.4 ± 0.3	17	4.9 ± 2.5	3.6 ± 0.8
Dayton	Aver.	–	–	28	11.6 ± 0.9	0.9 ± 0.4	18	1.1 ± 1.3	1.9 ± 0.4

† IC = inclusion. Grains were measured throughout the entire inclusion except for Carlton #3. Carlton #3a = edge; Carlton #3b = in phosphate.
± values indicate 1σ of compositional variability.
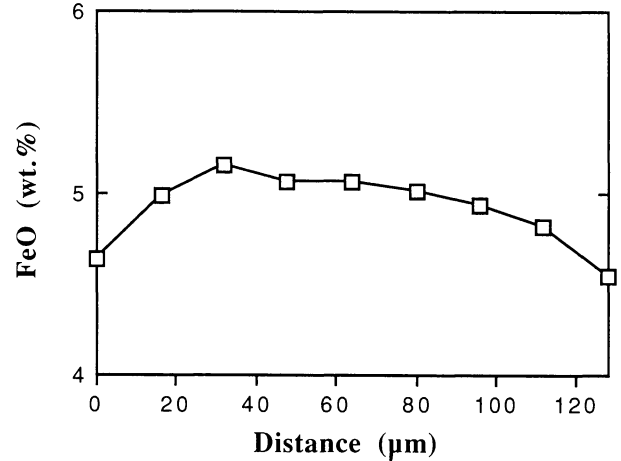N = Number of Analyses.

FIG. 4. Zoning profile across a large olivine grain from the silicate inclusion in Maltahöhe shown in Fig. 3. The grain exhibits inverse FeO zoning, indicative of solid-state reduction.

Inclusion Carlton #1 – This inclusion (Fig. 5a) consists of silicates (26.6 vol%; Table 1) and schreibersite (73.3 vol%) and is completely enclosed in a rim of swathing kamacite. A large (1mm long) olivine poikilitically encloses two orthopyroxene crystals and touches a smaller olivine. A plagioclase grain is detached from the olivine. Schreibersite almost completely surrounds and penetrates the large olivine grain. Two analyses each of olivine and pyroxene yield averages of $Fa_{6.6}$ and $Fs_{9.7}$, respectively, and plagioclase is $An_{0.8}Or_{4.1}$ (Table 2). A zoning profile across the large olivine grain (Fig. 6) reveals a nearly uniform composition.

Inclusion Carlton #2 – Silicates (55.6 vol%; Table 1), weathering products (16.5 vol.%) and the Fe,Ni-FeS intergrowth (6.7 vol%) are uniformly distributed, whereas schreibersite is found as a single, large grain at one end of the inclusion (Fig. 5b). Minor amounts of graphite (3.7 vol%) rim isolated silicate grains at the edge of the inclusion. Polycrystalline troilite is coarse-grained in a single occurrence. Phosphates were not observed, and kamacite surrounds the entire inclusion. Average mafic silicate compositions ($Fa_{6.6 \pm 0.2}$, N = 7; $Fs_{9.7 \pm 0.6}$, N = 8) are similar to those in Inclusion Carlton #1. A zoning profile across an olivine (Fig. 6) shows that FeO concentrations increase by ~ 0.5 wt% from the edge to the center of the grain. Plagioclase has an average composition of $An_{5.2 \pm 1.4}Or_{3.4 \pm 0.7}$.

Inclusion Carlton #3 – Phosphates comprise 70.3 vol% of the largest inclusion (Table 1, Fig. 5c). Chlorapatite is the dominant phosphate (69.8 vol%), with a new phosphate ($Na_2CaMg_7(PO_4)_6$) occurring as a volumetrically minor phase. This new phosphate occurs as an irregularly shaped grain at the boundary between chlorapatite and silicates at the edge of the inclusion. A description of this mineral, and compositional data on phosphates in Carlton and Dayton will be published elsewhere. Silicates (12.8 vol%) occur both in the phosphate and at the edge of the inclusion. Schreibersite and the Fe,Ni-FeS intergrowth occur at the edge of the inclusion which is rimmed by swathing kamacite.

Olivine compositions vary (Table 2), depending on the location of the individual grains. Grains within the phosphate ($Fa_{7.5 \pm 0.5}$, N = 3) are slightly higher in FeO than those at the

edge of the inclusion ($Fa_{6.7 \pm 0.3}$, N = 5). Zoning across an olivine grain from within the phosphate shows a flat profile at around 7.75 wt% FeO (Fig. 6). Pyroxenes ($Fs_{9.8 \pm 0.1}$ at the edge; $Fs_{9.5 \pm 0.4}$ in the phosphate) and plagioclase grains ($An_{6.3 \pm 3.3}Or_{3.3 \pm 0.9}$ at the edge; $An_{4.0 \pm 2.7}Or_{4.0 \pm 0.8}$ in the phosphate) show no significant compositional differences.

Dayton

Dayton (17.0 wt% Ni) is unique in containing an intimate mixture of a finest octahedral Widmanstätten pattern and pearlitic or lamellar plessite. The high C content detected by Moore *et al.* (1969) and the occurrence of pearlitic plessite in IA irons suggests that the pearlitic structure in Dayton is partly caused by high C concentrations (Buchwald, 1975; Kowalik *et al.*, 1988). Carbon appears to be irregularly distributed as Dayton contains a graphite-bearing nodule 4 x 4.5 x 5 cm in size (Buchwald, 1975; R. S. Clarke, Jr., pers. comm., 1993).

Phosphate-dominated inclusions containing pyroxene, plagioclase and minor (0.14%) SiO_2 have been described by Scott and Bild (1974), Fuchs *et al.* (1967) and Prinz et al. (1982). A notable feature of these inclusions is the absence of olivine. Fuchs *et al.* (1967) describe whitlockite, brianite and panethite and detected sphalerite in an X-ray powder pattern. Schreibersite is noted as rimming most inclusions.

The three silicate-bearing inclusions studied here comprise 18.2 vol% of section USNM 1592, which measures approximately 2.5 x 2.5 cm. The overall abundance of silicate-bearing inclusions in Dayton is much lower, however, and comprises at most a few vol%.

Like previous authors, we find pyroxene, plagioclase and SiO_2 in all three inclusions we studied. These minerals occur as mono- or poly-mineralic clusters in matrices of phosphates or schreibersite. SiO_2 occurs as a μm-sized intergrowth with troilite and pyroxene, usually bordering large troilite grains at the edge of the inclusions. Brianite and panethite are the dominant phosphates, with whitlockite present in one inclusion. Schreibersite and troilite occur at the edges of the inclusions. No graphite or carbides are observed within the silicate-bearing inclusions.

Inclusion Dayton #1–This 6.8 x 4.6 mm inclusion is dominated by phosphates (54.6 vol%, Table 1), with whitlockite, brianite and panethite occurring in subequal amounts (Fig. 7a). Silicates occur within or bordering panethite and brianite, and are never completely included within whitlockite. Troilite occurs as both small blebs within the inclusion and as large grains, together with schreibersite, sphalerite (600 μm) and metallic Cu (125 μm) at the edge of the inclusion. Large pyroxene grains, particularly those bordering large troilite

FIG. 5. Reflected light photomicrographs of inclusions in Carlton. A) Inclusion Carlton #1. The central part consists of silicates (S), including one large olivine which poikilitically encloses two orthopyroxene crystals, and separate smaller grains of olivine and plagioclase. Silicates are partially included in and, in one place, invaded by schreibersite (Sc), which exsolved from the metal. Swathing kamacite metal (M) encloses the entire assemblage and contains areas of terrestrial oxidation. Scale bar = 500 μm. B) Inclusion Carlton #2 is dominated by the silicates (S) olivine, pyroxene and plagioclase, which occur as polymineralic clusters in the center and as isolated grains on the edge of the inclusion. Graphite (Gr) rims many of these isolated grains. A shock-melted intergrowth (In) of troilite and Fe,Ni metal occurs throughout the inclusion, a large schreibersite (Sc) occurs at one end, and the entire inclusion is rimmed by swathing kamacite (M). This type of inclusion appears to be the most abundant, having also been described by Kracher and Kurat (1977) and Prinz *et al.* (1982). Scale bar = 1 mm. C) Inclusion Carlton #3. The dominant phase (~ 70 vol%) is chlorapatite (Cl), with a new Ca,Na,Mg-rich phosphate (NP) occurring at the edge. Silicates (S) are olivine, pyroxene and plagioclase and occur as mono- and polymineralic clusters within the chlorapatite and at the edge of the inclusion. Also at the edge are schreibersite (Sc) and an Fe,Ni-FeS intergrowth (In). The metallic host (M) includes a rim of swathing kamacite. This inclusion is very different from any previously recognized in Carlton. Scale bar = 2 mm.
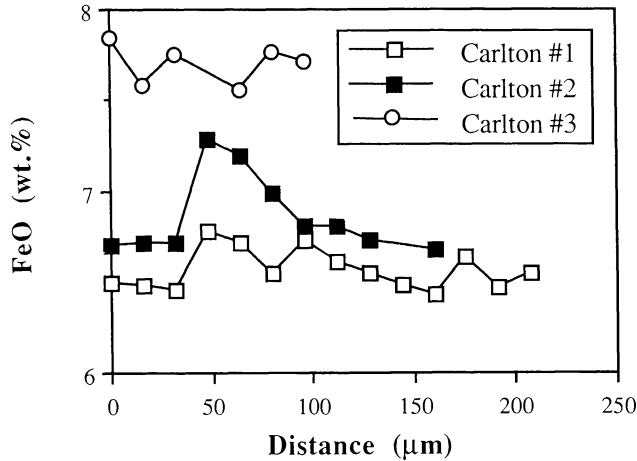
FIG. 6. FeO zoning profiles of olivine grains in Carlton. The largest olivine is from Inclusion Carlton #1 and is bordered by schreibersite. It has a flat profile and the lowest average FeO content. Olivine with intermediate FeO is from Inclusion Carlton #2 and is zoned. The smallest grain is included in chlorapatite in Inclusion Carlton #3, has a flat zoning profile and the highest average FeO content.

grains, often contain a myrmekitic intergrowth of SiO_2, troilite, and pyroxene. Pyroxene grains average $Fs_{11.8 \pm 1.0}$ (Table 2), and typically exhibit inverse zoning with FeO concentrations 1–1.5 wt% higher in the cores of the grains than at the rims. Plagioclase averages $An_{0.7 \pm 0.8}Or_{1.8 \pm 0.4}$, with a range from Ca-free albite grains to those with $An_{1.8}$. SiO_2 contains 0.6–0.8% FeO, and all other elements are below detection limits. Analyses of brianite, panethite and whitlockite agree well with those of Fuchs *et al.* (1967). Sphalerite $(Zn,Fe)S$ averages 22.0% Fe (N = 3). We have measured 1.19% Fe and 0.99% Ni (N = 3) in metallic Cu, although fluorescence of Fe from troilite or metal may be responsible for a portion of the apparent iron content (*c.f.*, Olsen, 1973).

Inclusion Dayton #2–This inclusion (Fig. 7b) is quite similar to Dayton #1. It contains silicates (5.5 vol%; Table 1) in a phosphate matrix of brianite and panethite (22.3 vol%). Of the three inclusions, the pyroxene-troilite-SiO_2 intergrowth is most abundant in this inclusion. Large schreibersite (53.7 vol%) and troilite (18.2 vol%) grains occur at the edge of the inclusion. Pyroxene has an average composition of $Fs_{11.5 \pm 0.7}$, while plagioclase is $An_{1.1 \pm 1.7}Or_{1.9 \pm 0.3}$. SiO_2 contains 0.21–0.97% FeO.

Inclusion Dayton #3–A single, large (4.5 mm) schreibersite grain (Fig. 7c) contains scattered pockets of pyroxene and plagioclase with or without included blebs of Fe,Ni metal and troilite, associated large troilite grains and brianite. Schreibersite accounts for 83.2 vol% of the inclusion (Table 1), silicates make up 12.7, troilite 3.3 and brianite 0.8 vol% of the inclusion. Pyroxene $(Fs_{11.6 \pm 0.8})$ and plagioclase $(An_{1.3 \pm 1.4}Or_{2.0 \pm 0.5})$ are similar in composition to those in other inclusions. Analyses of brianite agree well with those of Fuchs *et al.* (1967).

DISCUSSION

We now outline how inclusion mineralogy and mineral compositions change systematically with the Ni concentration of the metallic Fe,Ni hosts. These changes can be used to evaluate the models put forth for the genesis of IAB and IIICD irons.

Correlated Changes in Inclusion Mineralogy with Host Ni Concentration

Although interpretation of our data suffers from the low abundance of silicate-bearing IIICDs (only three are known), a relationship appears to exist between the Ni concentrations of the metal host and the mineralogy and composition of the phases in the silicate-bearing inclusions.

The FeO contents of mafic silicates in IIICDs increase with increasing Ni content of the host metal. This is shown for pyroxene in Fig. 8a, which illustrates Fs *vs.* host Ni for IIICDs and includes data for IABs, which show no such relationship (Bunch *et al.*, 1970; Scott and Bild, 1974; Wasson, 1970a,b). Pyroxenes in Maltahöhe are similar in composition to those of IABs, whereas those in Carlton and Dayton are significantly higher in Fs. Olivine Fa concentrations also increase with Ni concentration, although olivine is only present in Maltahöhe and Carlton.

An additional difference between IIICDs and IABs is noted in the plagioclase compositions: plagioclase in IIICDs is lower in An than that in IABs (Fig. 8b). Furthermore, An of plagioclase is not correlated with host Ni for either IIICDs nor IABs. The origin of this difference between IABs and IIICDs is uncertain. We do not, however, believe it is caused by reaction with phosphorus in IIICDs, since no phosphates are observed in Maltahöhe. It appears more likely that this difference is a primary feature of the precursor chondritic material.

The concentrations of oxidized phosphorus also change with Ni content of the host metal. The bulk phosphorus contents were calculated from measured mineral compositions and modal abundances (Table 1) for each inclusion. Schreibersite was excluded from these calculations since it is a later exsolution product and, thus, does not reflect chemical changes in the metallic magma. While inclusion-to-inclusion heterogeneity can be extreme, as shown by Carlton, the absence of phosphate in Maltahöhe and the abundant phosphates in Dayton suggests that the trend is real. We have considered the possibility that other inclusions in Maltahöhe could be phosphate-rich, but all other inclusions examined in hand sample seem to be dominated by graphite and troilite, not phosphates. Bulk P contents of Carlton and Dayton inclusions are 4.1 and 5.3 wt% P, respectively. No such relationships are apparent in the published data for IABs. Phosphate mineralogy also changes systematically with Ni content in the IIICDs. In Carlton, the dominant phosphate is chlorapatite, and the new Na,Ca,Mg-rich phosphate is a minor phase. In contrast, the Ca,Na,Mg-rich phosphates brianite and panethite are the dominant phosphates in Dayton. Available data on phosphates in IAB irons suggest that occurrence of unusual phosphates is not limited to high-Ni members: Although brianite occurs in the high-Ni (25%) San Cristobal iron (Scott and Bild, 1974), it has also been reported from Youndegin (Fuchs, 1969), one of the lowest-Ni members (6.38 wt%; Wasson, 1970a).

Silicate mineralogy also changes with increasing Ni of the metallic Fe,Ni: Maltahöhe and Carlton have olivine, pyroxene and plagioclase, whereas in Dayton, olivine is absent and SiO_2, pyroxene, and plagioclase are present. The texture of the SiO_2-troilite-pyroxene intergrowth in Dayton is similar to that observed in lunar rocks (*e.g.*, Roedder and Weiblen, 1974), where it has been attributed to sulfidization reactions between olivine and S gases. However, it is not clear if the occurrence in
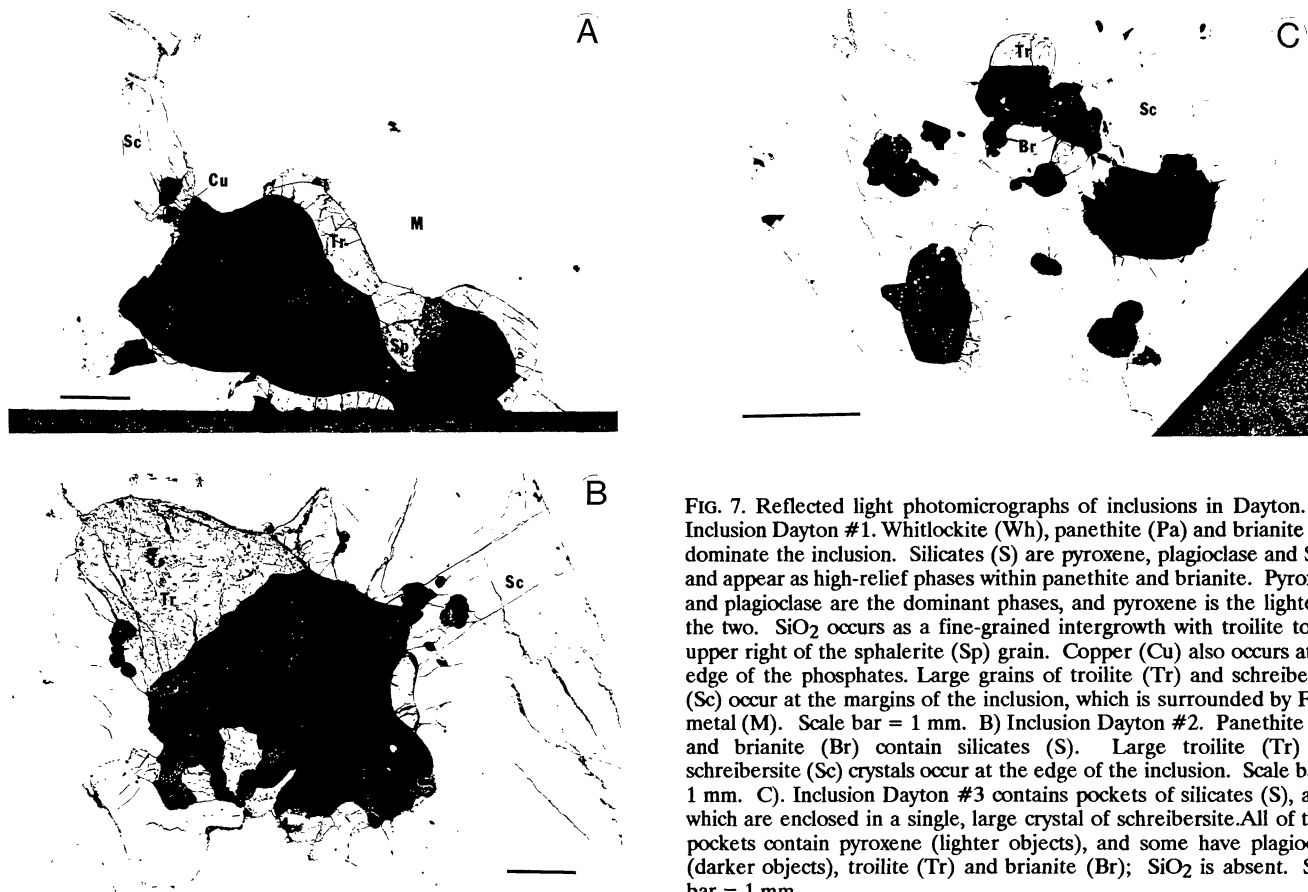
A

B

C

FIG. 7. Reflected light photomicrographs of inclusions in Dayton. A) Inclusion Dayton #1. Whitlockite (Wh), panethite (Pa) and brianite (Br) dominate the inclusion. Silicates (S) are pyroxene, plagioclase and SiO$_2$ and appear as high-relief phases within panethite and brianite. Pyroxene and plagioclase are the dominant phases, and pyroxene is the lighter of the two. SiO$_2$ occurs as a fine-grained intergrowth with troilite to the upper right of the sphalerite (Sp) grain. Copper (Cu) also occurs at the edge of the phosphates. Large grains of troilite (Tr) and schreibersite (Sc) occur at the margins of the inclusion, which is surrounded by Fe,Ni metal (M). Scale bar = 1 mm. B) Inclusion Dayton #2. Panethite (Pa) and brianite (Br) contain silicates (S). Large troilite (Tr) and schreibersite (Sc) crystals occur at the edge of the inclusion. Scale bar = 1 mm. C). Inclusion Dayton #3 contains pockets of silicates (S), all of which are enclosed in a single, large crystal of schreibersite.All of these pockets contain pyroxene (lighter objects), and some have plagioclase (darker objects), troilite (Tr) and brianite (Br); SiO$_2$ is absent. Scale bar = 1 mm.

Dayton formed in this way. For comparison, all IABs studied by Bunch *et al.* (1970) and Scott and Bild (1974) contain silicate assemblages of olivine, pyroxene and plagioclase, including that of the high-Ni (25%) IAB San Cristobal.

Finally, graphite content in the silicate-bearing inclusions appears to decrease with increasing Ni: The inclusion in Maltahöhe has 25.4 vol% graphite; one inclusion in Carlton contains 3.7 vol%, while the other two in Carlton and all in Dayton are graphite-free. A similar relationship may exist in IABs. Graphite appears to be more abundant in low-Ni than in high-Ni IABs. Bunch *et al.* (1970) classified the silicate inclusions of 11 IABs as either of the Odessa- (> 5% graphite) or the Copiapo-type (<5% graphite). Five of the meteorites with >8.5% Ni contain Copiapo-type inclusions, while the six with <8.5% Ni contain a mix of Odessa- and Copiapo-types. Thus, graphite content tends to decrease with increasing Ni content, although some scatter exists at low Ni contents. However, we do not know accurately the bulk carbon contents of these meteorites as graphite and carbides are heterogeneously distributed in IAB and IIICD irons (*e.g.*, Scott, 1971; Buchwald, 1975).

Constraints on Models for the Genesis of IIICD Irons

We find that four properties (*i.e.*, FeO contents of mafic silicates, concentrations of oxidized phosphorous, silicate mineralogy, graphite content) appear to vary with the Ni concentration of the host metal. Although each correlation is

weak, taken together the evidence for systematic changes in mineralogy and mineral compositions is strong. These correlations suggest that reactions between silicates and the metallic magma may have played a major role in determining the inclusion mineralogy and composition. The first three of these changes with Ni content are not observed in IAB irons, suggesting that IIICD and IAB irons had somewhat different origins. We discuss below both our own and previously published data in the context of mechanisms which may have formed or modified IIICD silicate-bearing iron meteorites. We discuss three processes that have previously been proposed for the origin of IIICD and IAB irons. These include oxidation-reduction (Scott and Bild, 1974), impact (Wasson *et al.*, 1980), and fractional crystallization of S-saturated cores (Kracher, 1982, 1985).

Oxidation-Reduction — It is clear that silicates in IIICDs have been effected by reduction. Silicates exhibit inverse zoning of FeO, and Fs contents of pyroxene are higher than Fa contents of olivine. These features have previously been attributed to solid-state reduction (*e.g.*, Kallemeyn and Wasson, 1985), and Seckendorff *et al.* (1992) have recently shown experimentally that these features cannot reflect thermodynamic equilibrium, but must result from reduction.

The increasing FeO content of the silicates with increasing Ni content of the metal might be explained by exchange of Fe between the oxidized and reduced states, as discussed by Scott and Bild (1974) for IAB irons. These authors rejected this model for IABs, based on the low abundance of silicates and a lack of
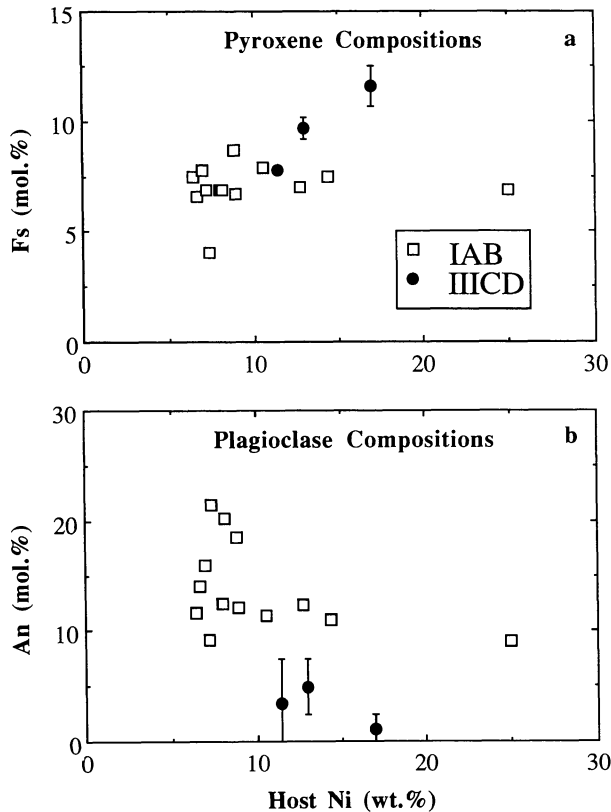
FIG. 8. Silicate mineral compositions *vs.* Ni contents in the host metal of IAB and IIICD irons. (data for IABs from Bunch *et al.*, 1970; Scott and Bild, 1974; Wasson, 1970a,b). Bars do not represent analytical uncertainties but reflect 1σ variability among all grains analyzed. A) Fs of pyroxene increases with increasing Ni for IIICDs, but no such trend is apparent for the IABs. Data for Maltahöhe, the lowest-Ni IIICD, are similar to the IABs. B) An of plagioclase in IIICDs is distinctly lower than that for IABs and neither shows a correlation with host Ni.

the composition of the metallic magma to change, particularly for those elements which probably interacted with the silicates (*e.g.*, S, C, P)? Below, we discuss these models in the light of these questions.

Impact Origin—Wasson *et al.* (1980) suggest that IAB and IIICD irons formed in individual melt pools in the megaregoliths of chondritic parent bodies from target materials of variable composition. Impact-induced partial melting is thought to have occurred at, or slightly above, the Fe,Ni-FeS eutectic (~920 °C to 1070 °C). The early, lower temperature melts would preferentially form from porous, Ni-rich sulfides and metal. These would be closest to the eutectic temperature and would crystallize under equilibrium conditions, producing high-Ni irons. Continuing impact-generated metamorphism destroyed the Ni-rich sulfides and metal. Thus, the Ni contents of the impact melts (and of the iron meteorites that crystallized from them) gradually decreased, forming the metal trends observed in IAB and IIICD irons. Wasson *et al.* (1980) propose that these materials were isolated from the parent rock, but they offer no explanation of how this melt migrated.

The Wasson *et al.* (1980) model does provide a straight forward solution to the problem of mixing silicates into the metallic magma. These materials could have been mixed during the same impact event that produced the metallic magma or by later shock-induced tectonism. In the former case, the silicates would be the parent material for the metallic magma, while in the latter case, the two are unrelated. It should be noted that no shock effects are observed in Maltahöhe, although we cannot exclude the possibility that such effects were annealed during slow cooling.

However, this model does not predict any of the trends observed in silicate inclusions in IIICDs. Wasson *et al.* (1980) state that the silicate inclusions found in these irons, to a large extent, preserve the composition of the parental material. They predict that high-Ni irons, which formed early in the history of the parent body, should preserve the unequilibrated silicate parent material. This is inconsistent with our observations. The high-Ni IIICD Dayton contains the most evolved silicate and phosphate assemblage, completely unlike that observed in chondrites. However, the arguments made by Wasson *et al.* (1980) were based on their knowledge of large, angular silicate clasts in IABs, not on the type of inclusion present in IIICDs and interactions between metallic magmas and silicates are possible in this scenario. However, a strong argument against the formation of these meteorites by impacts into parent body megaregoliths is the lack of similar stony-irons from, for example, the ordinary chondrite parent bodies. It is clear from the abundance of brecciated meteorites that the ordinary chondrite parent bodies experienced extensive impact bombardment from the very earliest time of the Solar System, yet no stony-irons of ordinary chondrite properties (*e.g.*, oxygen isotopic composition) exist. Additionally, no IAB stony-irons are younger than 4.48 Ga (Niemeyer, 1979b), although impacts certainly did not cease at this time.

Fractional Crystallization of a S-saturated core—Kracher (1982, 1985) proposes that metallic magmas are created by partial melting throughout the parent bodies at or near the Fe,Ni-FeS eutectic temperature. Migration of these melts to the centers of the parent bodies produces S-saturated cores. An important aspect of this model is that the entire column of residual material has essentially the same mineralogy and chemistry as the parent chondrite, only being depleted in FeS

correlation between FeO content in silicates and Ni content in the host metal, as would be predicted by such a model. In contrast, the FeO concentrations of the silicates in IIICDs increase as the Ni concentration of the metal increases, as expected from the oxidation-reduction model. However, the objection of low silicate abundances raised for IABs also holds for IIICDs: Silicates comprise at most a few percent of the bulk meteorite, too low to allow incorporation of all of the Fe that would have to be oxidized from the metal to account for the range of Fe/Ni ratios observed in the metal. Thus, although some reduction of silicates clearly took place, the oxidation-reduction model cannot account for the relationship between FeO concentration in the silicates and Ni concentrations in the host metal.

The remaining two processes (impact origin, Wasson *et al.*, 1980; fractional crystallization of S-saturated cores, Kracher, 1982, 1985) attempt to explain the formation of IAB and IIICD irons by formation of S-rich metallic magmas into which silicates are mixed, but in drastically different physical settings. We suggest that three major questions must be answered by any model for IIICD irons. First, how was the metallic magma formed and concentrated? Second, how were the silicates mixed into this metallic magma? Finally, what process caused

and, to a small extent, Fe,Ni metal. Thus, the silicate material like that found in IAB and IIICD irons existed immediately adjacent to the cores. Although heat sources are not explicitly discussed, the requirement for total parent body heating by Kracher (1985) suggests that he did not envision impacts as the major heat source.

Formation of S-saturated cores requires melt migration at small (≤ 5 vol%) partial melting. Kracher (1985) argued that at temperatures slightly above the eutectic, small degrees of silicate partial melting would open pathways and allow gravitational segregation of the Fe,Ni-FeS melts. While such migration can occur, gravity is probably not the dominant driving force. Partial melting experiments (Takahashi, 1983) suggest that at low degrees of partial melting, molten Fe,Ni and FeS form blebs which do not sink through the partially molten silicates. Indeed, partial melting may have to exceed 50% (Taylor, 1992; Taylor et al., 1993) for gravitational forces to drive melt migration. However, the depletion of Fe,Ni-FeS eutectic melts in lodranites, some of which experienced <10% partial melting, suggests that melt migration can occur at low degrees of partial melting (McCoy et al., 1993). Volatiles may have played an important role in driving Fe,Ni-FeS melts from their source regions (Keil and Wilson, 1993). If volatile inventories were sufficient to concentrate the Fe,Ni-FeS eutectic melt into large (e.g., tens of meters) veins, but insufficient to move this melt to the surface, the material in these large veins could sink to the center of the body, forming a S-saturated core. We have not, however, explored this possibility in detail.

Kracher (1982, 1985) suggests that impact-induced tectonism may have caused silicates and the metallic magma to mix at the core-mantle boundary. Several factors suggest that the postulated core-mantle boundary of the IAB and IIICD bodies was much more irregular than that of the IIIAB core (Haack and Scott, 1992). These factors include the low temperature and lack of partial melts in the silicate mantle and the small size of the core and corresponding low gravity. Smoothing of these irregularities in the core-mantle boundary may provide ample opportunity for metal-silicate mixing. Kracher (1985) notes that residual metal particles in the silicate portion of the parent body could sink into the lighter, S-rich core, carrying small amounts of adhering silicates. It appears, however, that this mechanism could only cause a very minute amount of silicates to be mixed into the mantle. Finally, Wasson et al. (1980) dispute that silicates mixed into a molten metallic core could retain abundant planetary gases. However, it is clear from the study of Acapulco (Palme et al., 1981) that chondritic rocks can remain at high temperatures for long periods of time and not lose their planetary gases.

Kracher (1982, 1985) has considered in some detail the crystallization of a S-saturated core. Initial crystallization produced the low-Ni cluster of IABs. At some point during the crystallization of the core, the melt would become S-saturated and crystallize both Fe-Ni metal and troilite. It is the crystallization of troilite which produces the differences between the IAB and IIICD irons and the other groups of irons. Kracher (1982) has estimated the general behavior of siderophile trace elements during co-crystallization of metal and troilite, reproducing the high-Ni tails of groups IAB and IIICD. It should be noted, however, that distribution coefficients for many elements in a S-rich system are unconstrained. Unfortunately, Kracher (1982) did not specifically address how the concentration of some elements that interacted with silicates (e.g., P, C, S) would change with crystallization. Jones and Drake (1983) point out that P is strongly enriched in the residual magma, even in S-rich melts, thus explaining the increasing phosphorus abundance with higher Ni content (increased fractional crystallization).

We suggest that other effects (e.g., nucleation effects, liquid immiscibility) played substantial roles in forming the IIICDs. Liquid immiscibility has been cited for creating carbon-rich (Kracher, 1985), S-rich (Kracher and Wasson, 1982) and P-rich (Jones and Drake, 1983) liquids. However, the extent of liquid immiscibility in determining the behavior of P, C and S has never been fully explored. Each of these elements is important in the magma of the IIICD iron parent body and probably formed one or more immiscible liquids. Inter-inclusion heterogeneity in Carlton, where one inclusion contains >70% phosphates and two inclusions are devoid of phosphates, may be due to liquid immiscibility. Solid silicates probably associate with one or more of these immiscible liquids, perhaps since both are buoyant in the core. Finally, we should not neglect the importance of nucleation effects. High graphite abundances in Maltahöhe inclusions may be due less to the high carbon content of the magma at that time than to the ease of nucleation of graphite on the associated silicates.

REFERENCES

BILD R. W. (1977) Silicate inclusions in group IAB irons and a relation to the anomalous stones Winona and Mt. Morris (Wis). *Geochim. Cosmochim. Acta* **41**, 1439–1456.

BOWEN N. L. AND SCHAIRER J. F. (1935) The system MgO-FeO-SiO₂. *Am. J. Sci.* **29**, 151–217.

BUCHWALD V. F. (1975) *Handbook of iron meteorites*. Univ. of California Press, Berkley, California. 1418pp.

BUNCH T. E., KEIL K. AND OLSEN E. (1970) Mineralogy and petrology of silicate inclusions in iron meteorites. *Contr. Mineral. Petrol.* **25**, 297–340.

CLAYTON R. N., MAYEDA T. K., OLSEN E. J. AND PRINZ M. (1983) Oxygen isotope relationships in iron meteorites. *Earth Planet. Sci. Lett.* **65**, 229–232.

FUCHS L. H. (1969) The phosphate mineralogy of meteorites. In *Meteorite Research* (ed. P. M. Millman), pp. 683–695. Reidel, Dordrecht, Holland.

FUCHS L. H., OLSEN E. AND HENDERSON E. P. (1967) On the occurrence of brianite and panethite, two new phosphate minerals from the Dayton meteorite. *Geochim. Cosmochim. Acta* **31**, 1711–1719.

GRAHAM A. L., ED. (1988) Meteoritical Bull. No. 66. *Meteoritics* **23**, 171–173.

HAACK H. AND SCOTT E. R. D. (1992) Asteroid core crystallization by inward dendritic growth. *J. Geophys. Res.* **97**, 14,727–14,734.

HINTENBERGER H., SCHULTZ L. AND WEBER H. (1969) Rare gases in the iron and in the inclusions of the Campo del Cielo meteorite, El Taco. In *Meteorite Research* (ed. P. M. Millman), pp. 895–900, Reidel, Dordrecht, Holland.

HOASHI M., VARELLA-ALVAREA H., BROOKS R. R., Reeves R. D., RYAN D. E. AND HOLZBECHER R. J. (1992) Revised classification of some

iron meteorites by use of statistical procedures. *Chem. Geol.* **98**, 1–10.

JONES J. H. AND DRAKE M. J. (1983) Experimental investigations of trace element fractionation in iron meteorites, II: The influence of sulfur. *Geochim. Cosmochim. Acta* **47**, 1199–1209.

KALLEMEYN G. W. AND WASSON J. T. (1985) The compositional classification of chondrites: IV. Ungrouped chondritic meteorites and clasts. *Geochim. Cosmochim. Acta* **49**, 261–270.

KEIL K. AND WILSON L. (1993) Explosive volcanism and the compositions of cores of differentiated asteroids. *Earth Planet. Sci. Lett.* **117**, 111–124.

KOWALIK J. A., WILLIAMS D. B. AND GOLDSTEIN J. I. (1988) Formation of the lamellar structure in group IA and IIID iron meteorites. *Proc. Lunar Planet. Sci. Conf.* **18th**, 493–501.

KRACHER A. (1982) Crystallization of a S-saturated Fe,Ni-melt, and the origin of iron meteorite groups IAB and IIICD. *Geophys. Res. Lett.* **9**, 412–415.

KRACHER A. (1985) The evolution of partially differentiated planetesimals: Evidence from iron meteorite groups IAB and IIICD. *Proc. Lunar Planet. Sci. Conf.* **15th**, C689–C698.

KRACHER A. AND KURAT G. (1977) Silicates in the Carlton (IIIC) iron meteorite and possible relations to group IAB (abstract). *Meteoritics* **12**, 282–283.

KRACHER A. AND WASSON J. T. (1982) The role of S in the evolution of the parental cores of the iron meteorites. *Geochim. Cosmochim. Acta* **46**, 2419–2426.

MALVIN D. J., WANG D. AND WASSON J. T. (1984) Chemical classification of iron meteorites–X. Multielement studies of 43 irons, resolution of group IIIE from IIIAB, and evaluation of Cu as a taxonomic parameter. *Geochim. Cosmochim. Acta* **48**, 785–804.

McCOY T. J., KEIL K., MUENOW D. W. AND WILSON L. (1993) Partial melting and explosive volcanism on the acapulcoite-lodranite parent body (abstract). *Meteoritics* **28** (in press).

MOORE C. B., LEWIS C. F. AND NAVA D. (1969) Superior analyses of iron meteorites. In *Meteorite Research* (ed. P.M. Millman), pp. 738–748. Reidel, Dordrecht, Holland.

NIEMEYER S. (1979a) I-Xe dating of silicate and troilite from IAB iron meteorites. *Geochim. Cosmochim. Acta* **43**, 843–860.

NIEMEYER S. (1979b) ^{40}Ar-^{39}Ar dating of inclusions from IAB iron meteorites. *Geochim. Cosmochim. Acta* **43**, 1829–1840.

OLSEN E. (1973) Copper-nickel alloy in the Blansko chondrite. *Meteoritics* **8**, 259–261.

PALME H., SCHULTZ L., SPETTEL B., WEBER H. W., WÄNKE H., CHRISTOPHE MICHEL-LEVY M. AND LORIN J. C. (1981) The Acapulco meteorite: Chemistry, mineralogy and irradiation effects. *Geochim. Cosmochim. Acta* **45**, 727–752.

PRINZ M., NEHRU C. E. AND DELANEY J. S. (1982) Silicate inclusions in irons and metal-silicate assemblages (abstract). *Lunar Planet. Sci.* **13**, 632–633.

RAMDOHR P. (1973) *The Opaque Minerals in Stony Meteorites.* Elsevier, Amsterdam. 245pp.

ROEDDER E. AND WEIBLEN P. W. (1974) Petrology of clasts in lunar breccia 67915. *Proc. Lunar Planet Sci. Conf.* **5th**, 303–318.

SCOTT E. R. D. (1971) New carbide, $(Fe,Ni)_{23}C_6$, found in iron meteorites. *Nature Physical Science* **229**, 61–62.

SCOTT E. R. D. AND BILD R. W. (1974) Structure and formation of the San Cristobal meteorite, other IB irons and group IIICD. *Geochim. Cosmochim. Acta* **38**, 1379–1391.

SECKENDORFF V. V., O'NEILL H. ST. C., ZIPFEL J. AND PALME H. (1992) Evidence for a late reducing event in IAB-silicate inclusions (abstract). *Meteoritics* **27**, 288.

SPRATT C. AND STEPHENS S. (1992) Against all odds: Meteorites that have struck home. *Mercury* **2**, 50–56.S

STÖFFLER D., KEIL K. AND SCOTT E. R. D. (1991) Shock metamorphism of ordinary chondrites. *Geochim. Cosmochim. Acta* **55**, 3845–3867.

TAKAHASHI E. (1983) Melting of a Yamato L3 chondrite (Y-74191) up to 30 Kbar. *Proc. Symp. Antarctic Meteorites* **8th**, 168–180.

TAYLOR G. J. (1992) Core formation in asteroids. *J. Geophys. Res.–Planets* **97**, 14,717–14,726.

TAYLOR G. J., KEIL K., McCOY T., HAACK H. AND SCOTT E. R. D. (1993) Asteroid differentiation: Pyroclastic volcanism to magma oceans. *Meteoritics* **28**, 34–52.

WASSON J. T. (1970a) The chemical classification of iron meteorites, IV. Irons with Ge concentrations greater than 190 ppm and other meteorites associated with group I. *Icarus* **12**, 407–423.

WASSON J. T. (1970b) Ni, Ga, Ge, and Ir in the metal of iron-meteorites-with-silicate-inclusions. *Geochim. Cosmochim. Acta* **34**, 957–964.

WASSON J. T. (1985) *Meteorites–Their Record of Early Solar-System History.* Freeman, New York, New York. 267 pp.

WASSON J. T. AND SCHAUDY R. (1971) The chemical classification of iron meteorites–V: Groups IIICD and IIID and other irons with germanium concentrations between 1 and 25 ppm. *Icarus* **14**, 59–70.

WASSON J. T., WILLIS J., WAI C. M. AND KRACHER A. (1980) Origin of iron meteorite groups IAB and IIICD. *Z. Naturforsch. A.* **35**, 781–795.

WLOTZKA F., ED. (1991) Meteoritical Bulletin No. 71. *Meteoritics* **26**, 255–262.